CERN - European Organization for Nuclear Research

LCD-Note-2013-005

Occupancy in the CLIC_ILD Time Projection Chamber using Pixelised Readout

Martin Killenberg*

* *CERN, Switzerland*

April 23, 2013

Abstract

The occupancy in the CLIC_ILD TPC caused by the beam induced background from $\gamma\gamma \rightarrow$ hadrons, e^+e^- pairs and beam halo muons is very high for conventional pad readout. We show that the occupancy for a pixelised TPC readout is moderate and might be a viable solution to operate a TPC at CLIC.

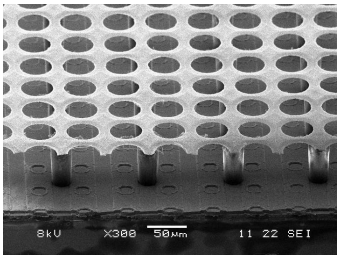

Figure 1: An InGrid detector consisting of a Timepix chip with 55 µm pixel pitch and the integrated grid, mounted by waver post-processing.

1 Introduction

The TPC occupancy studies for the CLIC conceptual design report [1] have been performed at 3 TeV centre-of-mass energy and for pad sizes of 1×6 mm^2, 1×4 mm^2 and 1×1 mm^2. While the voxel occupancies for 1×6 mm^2 and 1×4 mm^2 pads are very high, the 1×1 mm^2 pad size cannot be implemented with current technologies and would require further hardware R&D.

A promising option are pixel readout ASICs with a pixel size of $\mathcal{O}(100\ \mu\text{m})$ and an integrated micro mesh for gas amplification, so called InGrid chips [2]. A Micromegas-like gas amplification grid is placed on top of a pixel readout chip by means of wafer post-processing (figure 1). Like this the pillars and holes of the Micromegas grid are perfectly aligned with the readout pixels, which allows for a high and homogeneous detection efficiency over the full chip, even for single electrons [3]. Due to the much smaller size of the pixels compared to pads the occupancy is significantly reduced. In addition, the capability to detect and resolve every individual primary ionisation electron could lead to an improved tracking performance.

In this study we compare the occupancies for different pixel sizes to the occupancies for pads for a full bunch train of beam induced background at 3 TeV centre for mass energy in the CLIC_ILD detector. For the simulation 300,000 incoherent e^+e^- pairs from beamstrahlung and 3.2 $\gamma\gamma \rightarrow$ hadrons events per bunch crossing have been used[1)] and 312 bunch crossings have been overlayed at digitisation level. These values correspond to one CLIC bunch train at 3 TeV centre-of-mass energy without safety factor.

2 Simulation

To allow the occupancy study also for pixelised readout, which can resolve single primary ionisation electrons, the simulation chain has to have a sufficient level of detail. The full detector simulation Mokka [5] and the MarlinTPC toolkit [6], which was used for digitisation, provide this detailed simulation chain.

The primary charge deposition is simulated with Mokka using a step length limit in the order of the pixel size to have a realistic spacing of the primary electron clusters. Afterwards a

[1] For occupancy studies with pads in addition one beam halo muons per bunch crossing was used. Their contribution to the occupancy is small and negligible with respect to the uncertainties on the other background components [4].

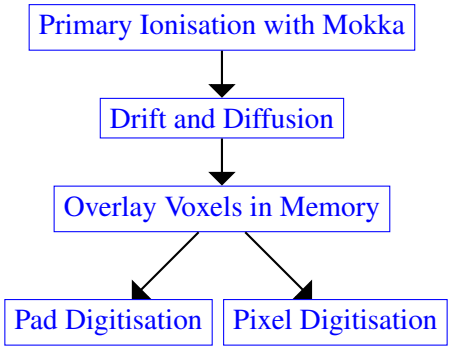

Figure 2: Overview of the simulation and digitisation chain.

displacement due to drift and diffusion is simulated separately for every primary electron. It is important to do this for individual electrons as 90 % of the clusters contain 3 electrons or less (most of them only one). A Gaussian smearing of a homogeneous charge would not be a good description for individual charges. To overlay all (background) events of the bunch train, the charge is filled into voxels (3D space buckets), so voxels which see charge from several events are not counted multiple times.

The digitisation is different for pads and pixels, as the simulated pixel readout ASIC only gives two values per pulse (the total charge and the average time), while the pad readout stores the measured ADC value for each time sample. However, in this simulation study an ADC recording all time samples per pixel has been used internally, featuring the same signal shaping time and readout frequency as the pad electronics for better comparison. This results in a "perfect" readout chip with unlimited multi-hit capability and very good pulse separation due to a fast shaping.[2)]

The gas amplification for pad readout simulates a triple GEM stack, including all details like collection and transfer efficiencies and gas gain fluctuations. For the InGrid-like chip a constant gas gain is used. The gain fluctuations are not relevant for the occupancy calculations, and for the tracking reported in section 4 the charge is not used and the data is interpreted as digital readout. A future dE/dx study would require the gas gain fluctuations to be implemented.

A short overview of the simulation chain is given in figure 2. A more in depth description can be found in a dedicated LCD note [7].

3 Occupancy With Pads And Pixels

3.1 Definitions

- **Pad/pixel occupancy**
  The pad or pixel occupancy is the number of pads/pixels with at least one active time

[2]Although an ASIC like this is unrealistic to be build in the foreseeable future, for this study it allows to study whether multi-hit capability or pulse height resolution are the more important feature.

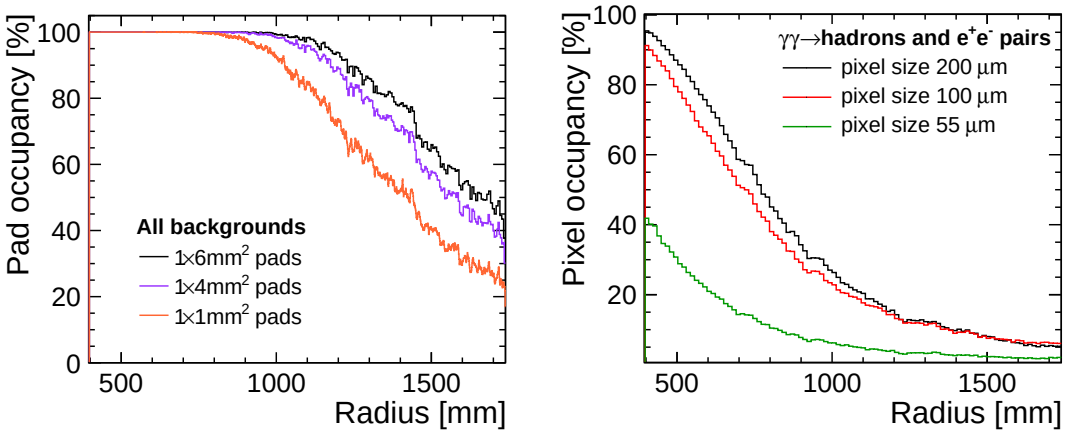

(a) The pad occupancy for different pad sizes.

(b) The pixel occupancy for different pixel sizes.

Figure 3: The two dimensional occupancy (fraction of active pads or pixels) for one bunch train of beam induced background at 3 TeV in the CLIC_ILD TPC as a function of the radius for different pad and pixel sizes.

sample during the bunch train, divided by the total number of pads/pixels.

- **Voxel occupancy**
  The voxel occupancy is the number of 3D readout cells (voxels) which see a signal, divided by all voxels in the TPC. A voxel has the size of a pad or pixel in the xy direction and the length of one time sample multiplied by the drift velocity in z direction. Due to the shaping of the electronics, a single pulse occupies several voxels, even if the signal is just on one channel. With a typical drift velocity of 79 mm/µs and a readout frequency of 40 MHz the voxel size in z is ≈ 2 mm.

3.2 Pad/pixel occupancy

The pad occupancy for 1×6 mm^2, 1×4 mm^2 and 1×1 mm^2 pads is shown in figure 3a. One can see that up to a radius of one metre basically all pads see a signal at some time during the bunch train. The pattern recognition truly has to be three dimensional as there almost certainly is a signal on the neighbouring pad. Even at the outer radius of the TPC the pad occupancy is 20 % to 40 %, depending on the pad size.

The pixel occupancy (figure 3b) for 100×100 µm^2 and 200×200 µm^2 is also above 90 % near the inner field cage of the TPC, but it drops quickly towards larger radii. For 55×55 µm^2 pixels the two-dimensional occupancy is only 40 % at the inner parts of the TPC, dropping to 2 % in the outer region. The high occupancy in the inner region shows that the readout ASIC should feature multi-hit capability and a short enough shaping time to allow a sufficient separation in the z direction.

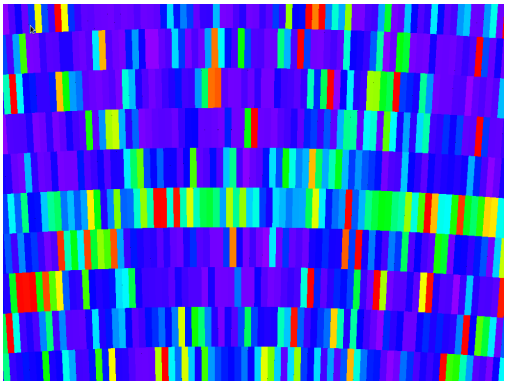

(a) 1×6 mm^2 pad size

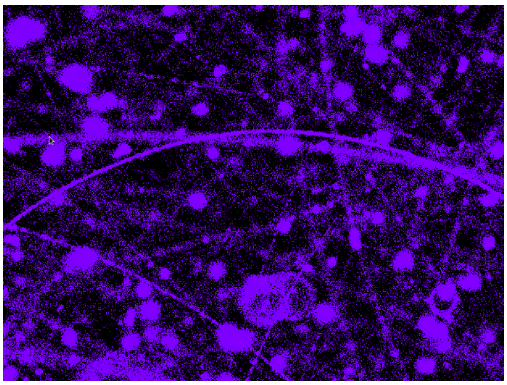

(b) 100×100 µm^2 pixel size

Figure 4: A section (approximately 75×60 mm^2 at a central radius of 550 mm) of the readout plane with signal from one bunch train of beam induced background at 3 TeV at CLIC, digitised with pad and pixel readout.

To visualise the difference between pixels and pads, figure 4 shows a section of the readout plane with one full CLIC bunch train of beam induced background, digitised with 1×6 mm^2 pads and 100×100 µm^2 pixels. While all the pads are occupied and almost no structure can be seen in this two-dimensional projection, the pixel readout allows to recognise individual particle tracks and many low energetic curlers.

3.3 Voxel occupancy

Figure 5a shows the average[3)] voxel occupancy in dependence on the radius for different pad sizes. The average three-dimensional occupancy for the largest pad size of 1×6 mm^2 is more than 30 % for the inner pad rows. Note that the occupancy does not scale linearly with the number of pads (i.e. the inverse of the pad size). This is a sign of saturation. The same voxel sees signals from different particle tracks, which causes ambiguities and can lead to inefficiencies in the reconstruction.

The voxel occupancy for pixel readout as a function of the radius is shown in figure 5b for three different pixel sizes. It is interesting to see that there is a factor four in the occupancies of 55×55 µm^2 and 100×100 µm^2 pixels, scaling (approximately) with the pixel size. This is an indication that there is no saturation when increasing the pixel size to 100 µm. The number of occupied voxels stays the same while the total number of voxels changes. However, going from 100×100 µm^2 to 200×200 µm^2 pixel size the occupancy increases only by a factor 1.3. This shows that the number of occupied voxels goes down by a factor 3, meaning that electrons which can be resolved individually with smaller pixels now end up in the same voxel. This is consistent with the expectation. With a transverse diffusion of 37 µm/$\sqrt{\text{cm}}$ and a mean distance between ionisation clusters of 350–400 µm the distances between individual electrons are expected to be

[3] Averaged over φ and z.

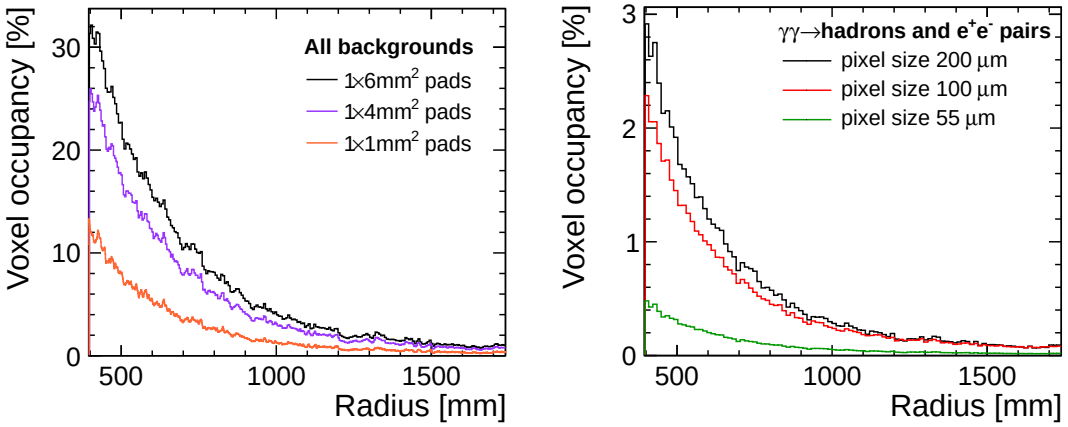

(a) The voxel occupancy for different pad sizes [4].

(b) The voxel occupancy for different pixel sizes.

Figure 5: The voxel occupancy of one bunch train of beam induced background at 3 TeV in the CLIC_ILD TPC as a function of the radius for different pad and pixel sizes.

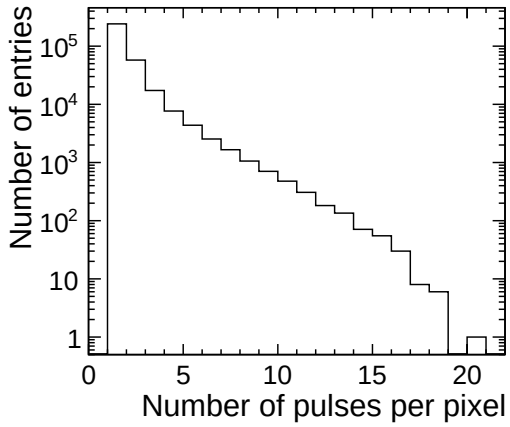

Figure 6: The number of pulses per pixel for a pixel size of 100×100 μm^2.

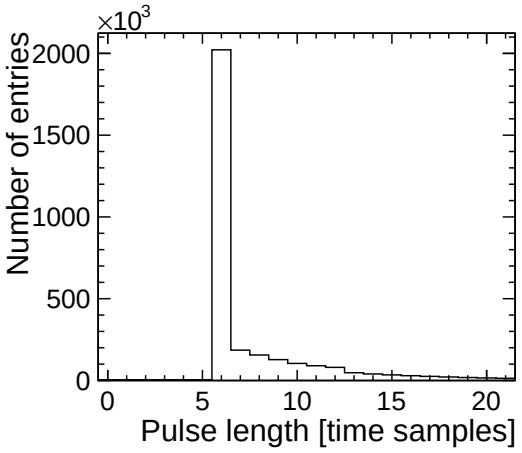

Figure 7: The pulse lengths for a pixel size of 100×100 μm^2 and a shaping time of 60 ns for the rising and the falling edge.

in the order of 200 μm.

Figure 6 shows the number of pulses per pixel for a pixel size of 100×100 μm^2. It shows an exponential behaviour, with 72 % of the pixels only having one pulse, and 94 % of the pixels seeing three pulses or less. This confirms the conclusion that individual electrons can be

resolved, as the probability of two pulses merging is very low with so few pulses per pixel.

The pulse length (number of time samples per pulse) for a pixel size of 100×100 µm^2 is shown in figure 7. Basically all pulses have a length of 6 time samples, which is determined by the electronics shaping. The simulation was done with a Gaussian shape and a shaping time (= 3 σ of the Gaussian) of 60 ns. For a sampling time of 25 ns this results in 6 time samples per pulse (including broadening due to the avalanche development in the gas amplification). If individual electrons can be resolved (as can be concluded from the occupancies), a charge measurement is not needed for each pulse. It would only measure the gas gain fluctuations. In this case a digital readout would be sufficient, which does not require an analogue shaping. If the charge on each pixel can be cleared within one time sample, the number of samples per pulse would be dominated by the development time of the charge amplification avalanche. In a Micromegas structure with a 50 µm amplification gap, as featured in the InGrid, the signal development time is $\mathcal{O}$(30 ns) [8]. One can conclude that the occupancy for a digital readout would be further reduced by a factor ≈3 compared to the simulated ASIC with analogue shaping.

4 Momentum Resolution With Pixel Readout

4.1 "Reconstruction"

To test the momentum resolution of the TPC, a track has to be reconstructed from the digitised data. For the pixel readout this brings the problem that there is no pattern recognition available yet. The pad based algorithms require contiguous and equidistant data in pad rows, which is not the case for the pixelised data. The Hough transform, which in principle is a working solution, breaks down for a full TPC because it is too slow.

For this study the pattern recognition has been skipped/cheated by associating all measured pixels to one track. Obviously this approach only works for single tracks without background.

For track fitting all pulses are treated equally, independent of their charge content ("digital readout"). A helix fit is performed on all the pixel positions of the track. δ electrons which propagate away from the track cause tails in the residual distribution. Figure 8 shows a δ electron which curls in the xy plane due to the electric field and propagates along z. The high hit density in the delta electron is an indication that a large amount of charge is deposited, but it is displaced from the original particle trajectory. For comparison the outline of 1×6 mm^2 pads is shown. With these the δ electron cannot be resolved, resulting in a hit with a large residual which can deteriorate the momentum resolution. In z the propagation of the δ electron is also clearly visible.

An iterative cut and refit procedure allows to reject outliers and δ electrons from the track fit. All hits with an residual larger than 2.5 times the RMS of the residual distribution are removed from the track and the track is refit. This procedure is repeated until it has converged. Figures 9 and 10 show the residual distributions of one single track in the xy plane and in z direction, respectively, both without and with the iterative cut for outlier rejection. Without cutting on the δ electrons there are tails and the peak is not centred around zero. The fact that one curling δ electron can affect the track fit so much that the peak is significantly shifted away from zero is caused by the equal treatment of all measured signals. After applying the outlier rejection, the tails are removed and the peaks are centred around zero.

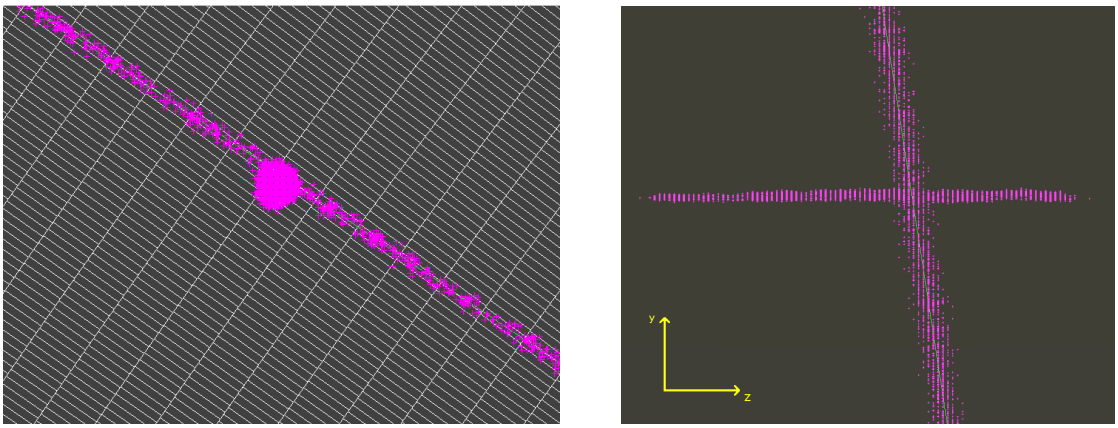

(a) *xy* projection. For comparison the shape of 1×6 mm^2 pads is shown.

(b) *zy* projection.

Figure 8: A single muon with 20 GeV transverse momentum in a 4 T magnetic field, digitised with a pixel size of 100×100 µm^2 pixels and 40 MHz readout frequency. As the time of the pulse is given as (integer) number of time samples by the digitiser, the 2 mm binning in z direction due to the time sampling is clearly visible. The δ electron propagates in positive and negative z direction. This is due to the fact that the z momentum is small compared to the transverse momentum. Collisions with gas atoms can flip the sign of the z momentum, so the δ electron can propagate in both directions.

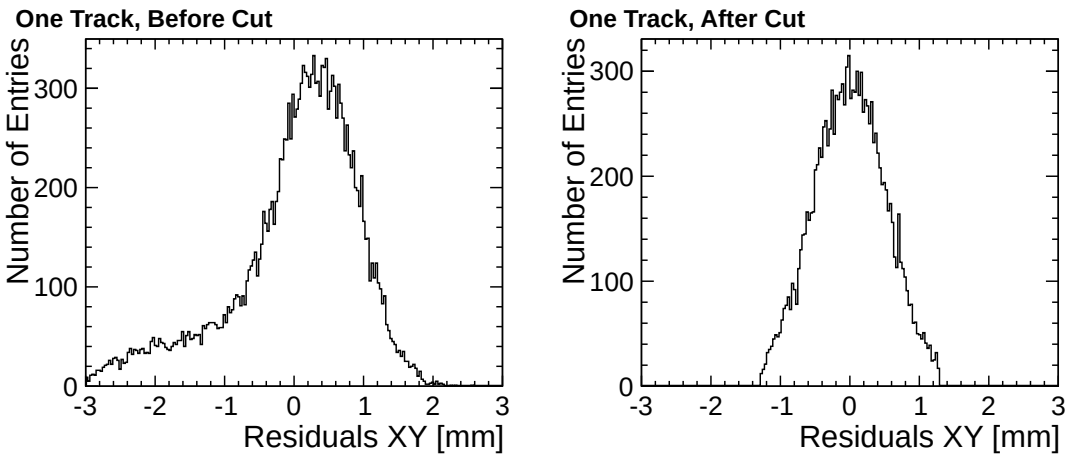

(a) The residual distribution including δ electrons.

(b) The residual distribution after the outlier rejection.

Figure 9: The residuals in the *xy* plane of one simulated track without and with the iterative outlier rejection cut.

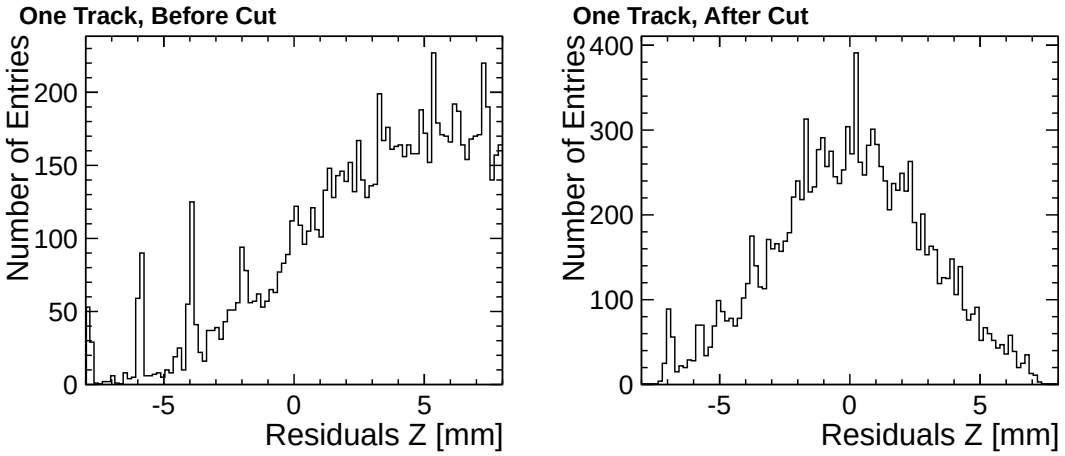

(a) The residual distribution including δ electrons.

(b) The residual distribution after the outlier rejection.

Figure 10: The residuals in z direction of one simulated track without and with the iterative outlier rejection cut. The equidistant spikes in the distribution are caused by the z binning in the curling δ electron.

4.2 Momentum resolution

To determine the momentum resolution 1000 muons have been simulated for each of seven transverse energies between 2 GeV and 200 GeV. The simulation is done using Mokka and the CLIC_ILD detector model with tracks at an angle of $\theta = 85^\circ$, so the tracks are near the cathode. The data are digitised with a pixel size of 100×100 µm^2 and reconstructed using the iterative helix fit with outlier rejection. A Gaussian has been fitted to the $\Delta p_\mathrm{T}/p_\mathrm{T}^2$ distribution and its σ is quoted as the resolution.

To compare the results with pad data, the Mokka simulation output has also been reconstructed with the default simulation and reconstruction chain used for tracking studies in the CLIC CDR, which is Mokka using 1×6 mm^2 pads and MarlinReco [9, 10]. It uses a Kalman filter for the track fitting to take energy losses into account.

Figure 11 shows the momentum resolution as a function of the transverse momentum, simulated for pad and pixel readout. One can see that the momentum resolution of the pixel readout with the simple helix fit is slightly better than the momentum resolution with pad readout, even though the latter uses a Kalman filter. This shows that the expected track momentum resolution of a pixel readout will at least be equal to the pad readout, once a pattern recognition is available. Probably using a Kalman filter in combination with pixel readout and δ electron rejection can result in even better performance.

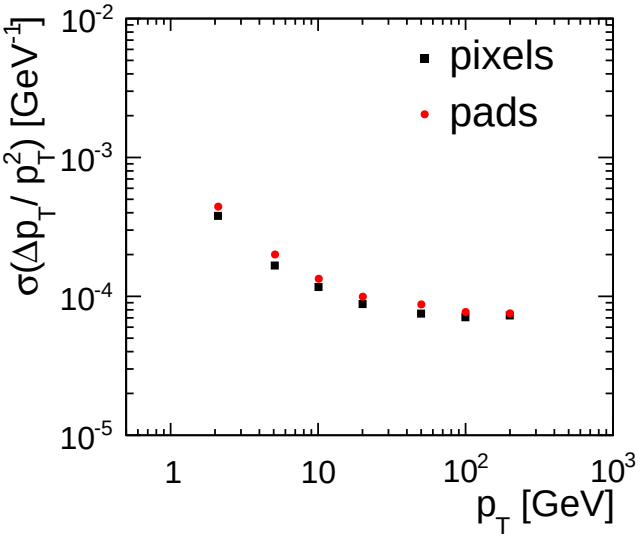

Figure 11: The track momentum resolution as a function of the transverse momentum for tracks at $\theta = 85^\circ$ in the CLIC_ILD detector, simulated for 1×6 mm^2 pads and 100×100 µm^2 pixel readout.

5 Conclusions

We simulated an ILD-like TPC with InGrid pixel readout and studied the occupancy for one bunch train of beam induced background for CLIC at 3 TeV centre of mass energy. The pixel occupancy (fraction of active pixels) is very high: More than 90 % for 100×100 µm^2 and 40 % for 55×55 µm^2 pixel size near the inner field cage. This shows that the chip should feature multi-hit capability and a short shaping time for good pulse separation.

The simulation with a multi-hit capable ASIC with fast shaping time shows a significantly reduced voxel occupancy (three-dimensional occupancy) of two percent for 100×100 µm^2 pixels at the inner radii, compared to 30 percent for the baseline design with 1×6 mm^2 pads. For smaller pixels the voxel occupancy scales linearly with the pixel size, indicating that single primary ionisation electrons are resolved. In this case the charge information per hit becomes irrelevant, only measuring the gas gain fluctuations in the Micromegas grid. The conclusion is that a digital readout ASIC is sufficient for a TPC at CLIC, but it should feature multi-hit capability and fast shaping for a good hit separation.

The high spatial resolution of such a readout allows for an effective suppression of δ electrons. The resulting momentum resolution for a simple helix fit is already better than the Kalman filter based approach in MarlinReco for pad readout. With these features the pixel readout is a promising candidate for a TPC readout in high occupancy environments. The high amount of data this produces and the current lack of a pattern recognition require further study to make it a viable option.

References

[1] L. Linssen, A. Miyamoto, M. Stanitzki, and H. Weerts, eds. *Physics and Detectors at CLIC: CLIC Conceptual Design Report*. CERN, 2012. ANL-HEP-TR-12-01, CERN-2012-003, DESY 12-008, KEK Report 2011-7, arXiv:1202.5940.

[2] M. Chefdeville, et al. An electron-multiplying 'Micromegas' grid made in silicon wafer post-processing technology. *Nucl.Instrum.Meth.*, vol. A556 pp. 490–494, 2006.

[3] M. A. Chefdeville. *Development of Micromegas-like Gaseous Detectors Using a Pixel Readout Chip as Collecting Anode*. Ph.D. thesis, University of Amsterdam, 2009.

[4] M. Killenberg. Occupancy in the CLIC_ILD Time Projection Chamber. CERN LCD-Note-2011-029, 2011.

[5] Mokka, a detailed Geant4 simulation for the International Linear Collider detectors. Website: http://ilcsoft.desy.de/portal/software_packages/mokka/.

[6] MarlinTPC, Marlin based simulation, digitisation, reconstruction and analysis code for the TPC. Website: http://ilcsoft.desy.de/portal/software_packages/marlintpc/.

[7] M. Killenberg. Software and parameters for detailed TPC studies in the CLIC CDR. LCD-Note-2011-025, 2011.

[8] I. Giomataris. MICROMEGAS: Results and prospects. *ICFA Instrum.Bull.*, vol. 19 p. 1, 1999.

[9] MarlinReco, a Marlin based reconstruction software. Website: http://ilcsoft.desy.de/portal/software_packages/marlinreco/.

[10] A. Raspereza. LDC Tracking Package. 2007. Proceedings of the 2007 International Linear Collider Workshop (LCWS07 and ILC07), Hamburg, Germany, http://www.slac.stanford.edu/econf/C0705302/papers/Sim10.pdf.